Tetrahedron 65 (2009) 2307–2312

Contents lists available at ScienceDirect

Tetrahedron

journal homepage: www.elsevier.com/locate/tet

An NBD-based colorimetric and fluorescent chemosensor for Zn^{2+} and its use for detection of intracellular zinc ions

Zhaochao Xu [a], Gun-Hee Kim [b], Su Jung Han [a], Min Jung Jou [a], Chongmok Lee [a,*], Injae Shin [b,*], Juyoung Yoon [a,c,*]

[a] Department of Chemistry and Nano Science, Ewha Womans University, Seoul 120-750, Republic of Korea
[b] Department of Chemistry, Yonsei University, Seoul 120-749, Republic of Korea
[c] Department of Bioinspired Science, Ewha Womans University, Seoul 120-750, Republic of Korea

ARTICLE INFO

Article history:
Received 5 December 2008
Received in revised form 8 January 2009
Accepted 8 January 2009
Available online 14 January 2009

ABSTRACT

A new 7-nitrobenz-2-oxa-1,3-diazole (NBD) based colorimetric and fluorescence chemosensor for Zn^{2+}, an ion involved in many biological processes, was designed and synthesized. The NBD-probe **1** displays a red-to-yellow color change and an enhancement of fluorescent intensity in the presence of an aqueous solution of Zn^{2+} ions (pH 7.2). Internal charge transfer (ICT) and photoinduced electron transfer (PET) mechanisms are responsible for these changes. The practical use of this probe was demonstrated by its application to the biologically relevant detection of Zn^{2+} ions in pancreatic β-cells.

1. Introduction

The ability to detect metal ions with high specificity under physiological conditions is an important criterion that must be met in the design of fluorescent chemosensors for biological and environmental applications.[1] In particular, the development of a fluorescent probe for zinc ion in the presence of a variety of other metal ions has received great attention. These efforts are stimulated by the fact that Zn^{2+} is involved in a variety of physiological and pathological processes. For example, Zn^{2+} is an essential component of many enzymes and it is involved in maintaining key structural features of gene transcription proteins.[2] Interestingly, in comparison with other tissues, high concentrations of Zn^{2+} are present in pancreatic islets, which play a critical role in insulin biosynthesis, storage, and secretion.[3] A decrease in the concentration of Zn^{2+} causes a reduction of the ability of the islet cells to produce and secrete insulin.[4] It is also reported that zinc ion is a potent killer of neurons via oxidative stress, the cause of neurodegenerative disorders.[5] Owing to the biological significance of zinc, a considerable effort has been devoted to the development of efficient and selective methods to detect Zn^{2+}.

Fluorescence based chemosensors have a key advantage over those that rely on other detection techniques, such as atomic absorption, X-ray fluorescence, and radioisotopes, in that they can be used to readily detect intracellular ion levels without the need for sophisticated instrumentation or time-consuming sample preparation.[1,6] Moreover, a dual colorimetric-fluorescent probe combines the sensitivity of fluorescence with the convenience and esthetic appeal of a colorimetric assay.[7]

Several fluorescent probes, such as Zinquin and 6-methoxy-8-quinolyl-*p*-toluenesulfonamide (TSQ), have been designed for the detection of intracellular zinc ions.[6a,b] However, these probes have relatively low selectivities for zinc ion in that they also respond to calcium ions. Therefore, the search continues for a Zn^{2+} fluorescent probe that has improved selectivity. Additional criteria applied in the design of these probes include ready synthesis, easy detection, good water solubility, high cell permeability, and long wavelength absorbance to avoid cell damage, and a high fluorescence background.

7-Nitrobenz-2-oxa-1,3-diazole (NBD) has been widely utilized as a fluorophore in various fluorescent chemosensors owing to its emission at long wavelengths and good cell permeability.[8] However, only one example of an NBD-based Zn^{2+} fluorescent probe has been described to date.[9] Although, not applied to monitor intracellular zinc ions, this PET mechanism based chemosensor shows a high selectivity and sensitivity for Zn^{2+} in aqueous solution with a significant 'off–on' fluorescence response.

Below, we describe the results of a study that has led to the development of the NBD-based probe **1**, which displays a red-to-yellow color change and a selective fluorescent enhancement in aqueous solutions (pH 7.2) containing Zn^{2+}. A combination of PET (photoinduced electron transfer) and ICT (internal charge transfer) processes are involved in promoting the color and fluorescence

* Corresponding authors. Tel.: +82 2 3277 2400; fax: +82 2 3277 2384 (J.Y.).
E-mail addresses: cmlee@ewha.ac.kr (C. Lee), injae@yonsei.ac.kr (I. Shin), jyoon@ewha.ac.kr (J. Yoon).

0040-4020/$ – see front matter © 2009 Elsevier Ltd. All rights reserved.
doi:10.1016/j.tet.2009.01.035

changes. By using NMR titration as well as cyclic voltammetry (CV) experiments, we have demonstrated that a unique stepwise binding mechanism is involved in this system. Furthermore, we have shown that **1** has excellent cell permeability. This conclusion comes from the observation that zinc ions present in pancreatic β-cells can be efficiently detected.

2. Results and discussion

The route used to synthesize **1** is initiated by coupling of *N*,*N*′-bis(2-pyridylmethyl)-ethane-1,2-diamine (**3**)[10] and NBD–Cl (**4**) to produce **2** in 86% yield (Scheme 1). Reaction of **2** with 2-(bromomethyl)pyridine under basic conditions gives **1** in 92% yield. The detailed procedures and spectroscopic characterization of products are given in the Experimental section and Supplementary data. By using this route, the complicated synthesis of the Zn^{2+} chelator *N*-bis-pyridin-2-ylmethylethane-1,2-diamine is circumvented.[9] It is worth mentioning that synthetic pathway we have developed can be applied to the preparation of diverse derivatives of **1**.

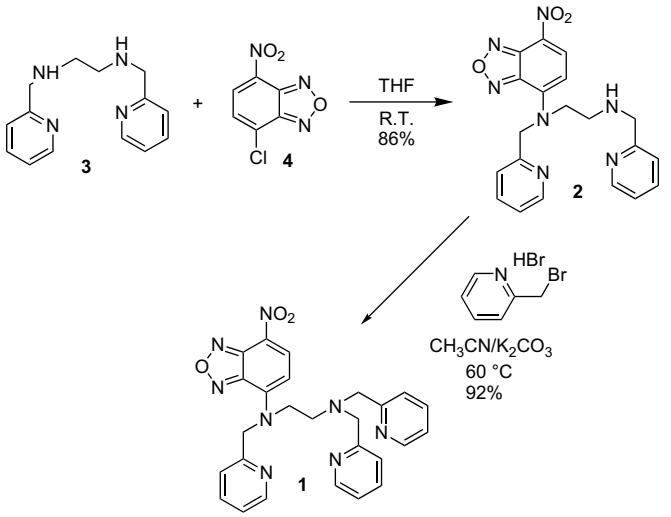

Scheme 1. Synthesis of compound **1**.

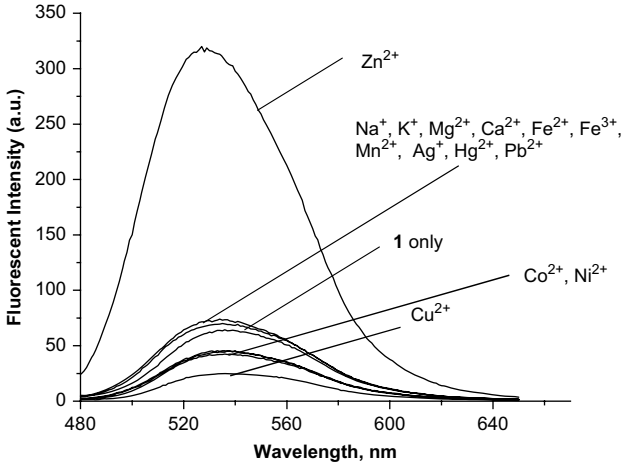

Figure 1. Fluorescent responses of a probe **1** (10 μM) to various metal ions (30 μM) in HEPES buffer (0.1 M, pH 7.2) (excitation wavelength: 470 nm, emission wavelength: 537 nm).

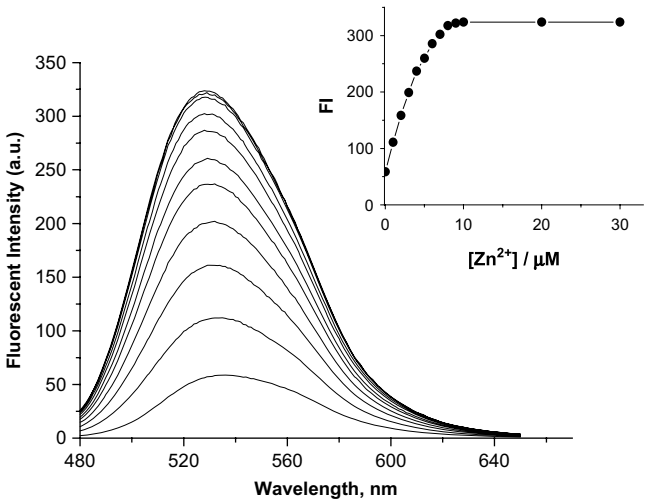

Figure 2. Fluorescent emission spectra of **1** (10 μM) in the presence of different concentrations of Zn^{2+} (0, 1, 2, 3, 4, 5, 6, 7, 8, 9, 10, 20, and 30 μM) in HEPES buffer (0.1 M, pH 7.2). Inset: a lot of the fluorescent intensity as a function of Zn^{2+} concentration.

The selectivity of the fluorescent response of **1** to zinc ion was probed initially. The addition of Zn^{2+} (3 equiv) to **1** (10 μM) in 100% aqueous solution (0.1 M HEPES, pH 7.2) causes a large CHEF (chelation enhanced fluorescence) (Fig. 1). In contrast, other metal ions do not promote changes in the fluorescence of **1**. More importantly, this probe does not respond to Ca^{2+}, a problem associated with other Zn^{2+} sensors. Fluorescence titration experiments show that the dissociation constant (K_d) of **1** with Zn^{2+} is 1.3±0.13 μM and **1**–Zn^{2+} adduct of 1:1 stoichiometry is formed (Fig. 2).[11] Additional studies showed that the binding of **1** to zinc ions is not affected by even high concentrations of calcium ions (Fig. 3).

The 'off–on' enhancement and slight blue shift of the fluorescence of probe **1** caused by Zn^{2+} is attributed to the operation of a combination of PET (photoinduced electron transfer) and ICT (internal charge transfer) processes.[1b] It is known that fluorophores containing an electron-donating group (often an amino group) and an electron-withdrawing group undergo ICT from the donor to the acceptor following electronic excitation. Photoinduced ICT, involving an electron-rich moiety of the fluorophore (e.g., an amino group) involved in interaction with a cation, causes the formation of a partial positive charge at a site adjacent to the cation. This change can affect the electronic absorption properties of

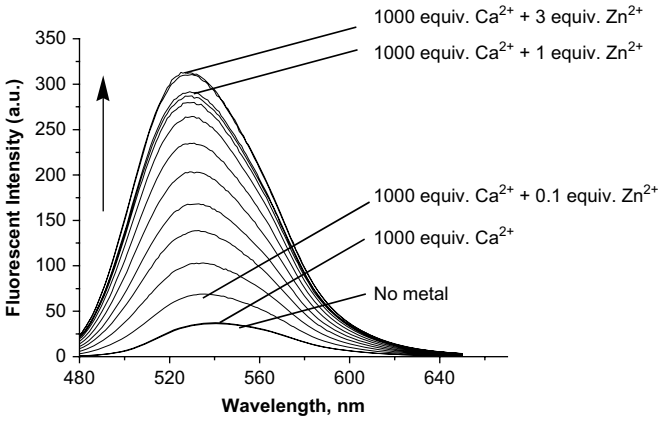

Figure 3. Effect of calcium ion on the binding of zinc ion to **1**. Zinc ions (0–3 equiv) were added to solutions of **1** (10 μM) containing a large excess of calcium ions (1000 equiv) in 0.1 M HEPES buffer (pH 7.2).

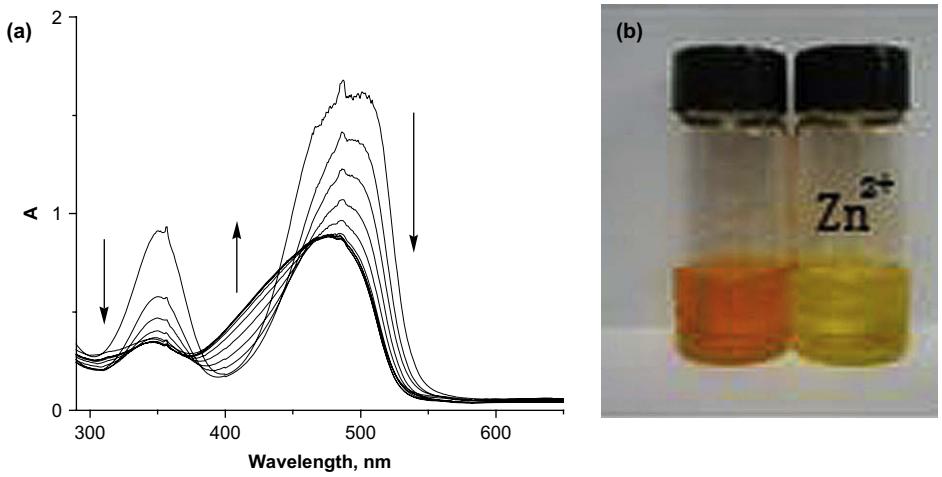

Figure 4. (a) Absorption spectra of **1** (100 μM) in the presence of different concentrations of Zn^{2+} (0, 10, 20, 30, 40, 50, 60, 70, 80, 90, 100, 200, and 300 μM) in HEPES buffer (0.1 M, pH 7.2). (b) Colorimetric change of **1** (100 μM) with Zn^{2+} (300 μM) in HEPES buffer.

a fluorophore with an ICT excited state. Specifically, a cation-induced blue shift in the absorption maximum is expected. Fluorescence emission properties are less affected by ICT in excited states.[5d] As a result, the fluorescence enhancement of **1** caused by Zn^{2+} is most likely associated with metal ion coordination to the nitrogen donor, which blocks PET quenching of the singlet excited state of the 7-nitrobenz-2-oxa-1,3-diazole moiety. Substantial changes in the absorption spectra of **1** take place upon addition of Zn^{2+}. The intensities of the absorption bands of **1** at 350 nm and 487 nm decrease upon addition of Zn^{2+} with the concurrent growth of a band at ca. 400 nm, corresponding to a colorimetric change (from red to yellow) that is clearly observable (Fig. 4).

These observations indicate that the blue shift in the UV absorption spectra and the enhanced fluorescence of **1** promoted by zinc ions are caused by the operation of a combination of ICT and PET mechanisms resulting from coordination of chelating

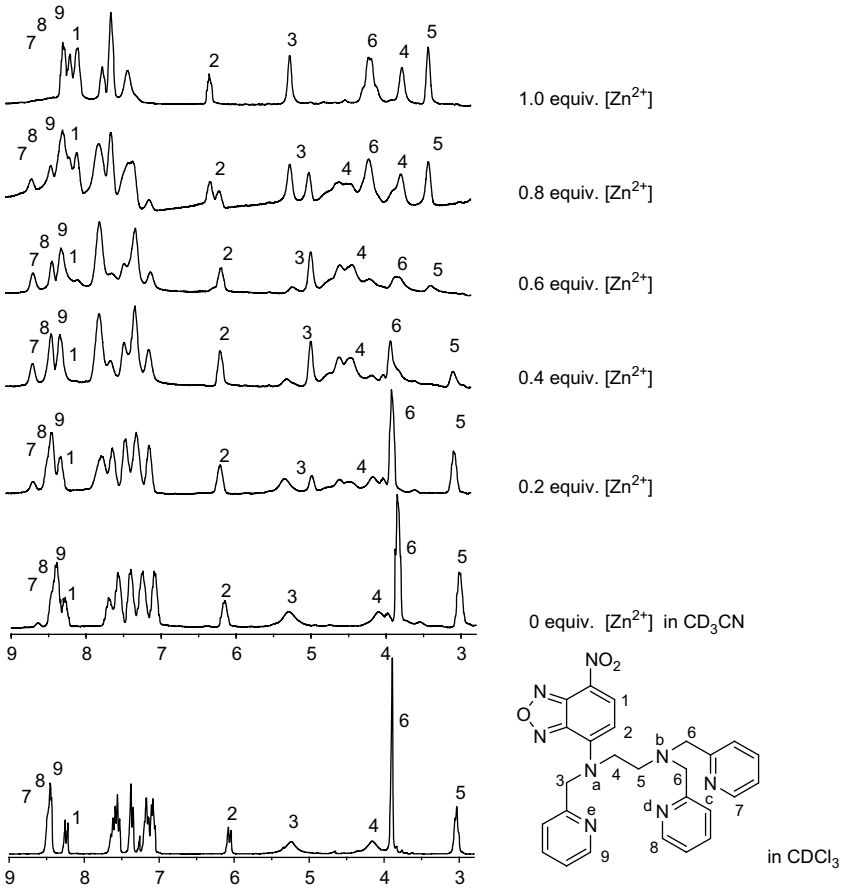

Figure 5. Partial ^1H NMR spectra of **1** (1 mM) in the presence of a different amount of Zn^{2+} in CD_3CN.

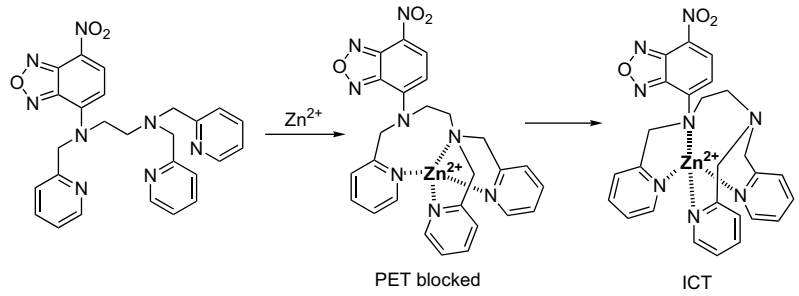

Scheme 2. Proposed mechanism of stepwise binding mode of **1** with Zn^{2+}.

nitrogens to Zn^{2+} (vide infra, electrochemical results). This proposal gains support from the results of NMR titration experiments (Fig. 5). Upon addition of 0.6 equiv of zinc, proton 2 in **1** undergoes only a slight chemical shift change, while resonances for protons 1 and 3–9 undergo significant changes. This finding is attributed to the proposed stepwise binding of **1** with Zn^{2+}, involving an early stage in which the four nitrogens N_b–N_e coordinate to Zn^{2+} and a final stage where N_a joins the receptor at the expense of the interaction between N_b and Zn^{2+}. At this point, PET from N_b to the NBD fluorophore is not blocked completely, explaining why the fluorescence enhancement of probe **1** is not large. The data in Figure 2 demonstrate that addition of 0.6 equiv Zn^{2+} induces a PET-blocked response associated with a large and gradual fluorescence enhancement, and that addition of the final 0.4 equiv Zn^{2+} promotes an ICT response that only slightly affects the fluorescence enhancement and wavelength shift.

The proposed mechanisms associated with zinc binding to **1** are shown in Scheme 2. When **1** interacts with Zn^{2+}, the resonance for proton 2 in **1** experiences a large downfield shift from 6.15 to 6.30 ppm due to the reduction of electron-donating ability of N_a, indicating the dynamic nature of the zinc sensing process.

To gain additional support for the mechanisms proposed for the binding process, changes in the electrochemical properties of **1** upon complexation with zinc were investigated by using cyclic voltammetry (CV). The results are shown in Figure 6, where the potentials of the redox waves for scans in the positive and negative directions are denoted as E_{ox} and E_{red}, respectively. Comparing the cyclic voltammograms of NBD–NH_2 with **1** shows that two new oxidation waves of **1** at E_{ox} of 1.03 V and 1.37 V can be ascribed to an *N*,*N*′-bis(2-pyridylmethyl)-ethane-1,2-diamine moiety (Fig. 6a and b). The results of the CV experiments demonstrate that the oxidation peak at E_{ox} of 1.03 V decreases dramatically upon addition of 0.4 equiv of Zn^{2+} without a decrease of the E_{ox} of 1.37 V (Fig. 6c). The oxidation peak at E_{ox} of 1.37 V nearly completely disappears upon further addition of up to 0.8 equiv of Zn^{2+} (Fig. 6d). In contrast, the two step change caused by Zn^{2+} is not observed in the CV of **1** with Ca^{2+}, where the oxidation peak at E_{ox} of 1.37 V remains intact (Fig. 6e). It was also found that the differences in '$E_{ox}-E_{red}$' values between **1** and '**1**+Zn^{2+}' are large. The E_{ox} of **1** is changed from 1.03 V to 1.72 V and E_{red} from −0.94 V to −0.52 V upon addition of 1.0 equiv of Zn^{2+}. This corresponds to a 0.27 eV increase in the '$E_{ox}-E_{red}$' value upon complexation of **1** with Zn^{2+}. Since the E_{ox} and E_{red} values are known to be related to the HOMO and LUMO energy levels, respectively,[12] the results show that the HOMO–LUMO energy gap in **1** is greatly altered upon binding of to zinc ions. Overall, we believe that CV data provide firm support to the operation of a combination of ICT and PET mechanisms in governing the colorimetric and fluorescence responses of **1** promoted by Zn^{2+}.

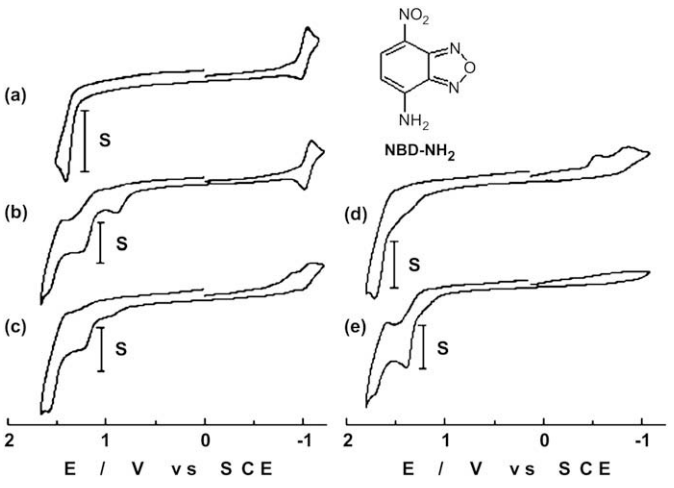

Figure 6. Cyclic voltammograms of (a) 1 mM NBD–NH_2, (b) **1**, (c) **1**+0.4 equiv Zn^{2+}, (d) **1**+0.8 equiv Zn^{2+}, and (e) **1**+1.0 equiv Ca^{2+} at a platinum disk electrode; in CH_3CN containing 0.1 M $TBAPF_6$; ν=0.1 V/s. The scale bar represents 10 μA.

The ability of **1** to detect intracellular zinc ions was also examined in this study. For this purpose, Neuro-2a neuroblastoma cells were cultured in Dulbecco's modified Eagle's medium (DMEM), supplemented with 10% FBS at 37 °C. The cells were incubated with 100 μM Zn^{2+} in culture media for 20 min at 37 °C. After washing with PBS to remove the remaining extracellular zinc ions, the cells were incubated with 100 μM **1** in culture media for 30 min at 37 °C. Analysis of the emission properties of the cells reveals that chemosensor **1** has cell permeability and that it fluorescently responds to intercellular zinc ions (Fig. 7a).

Owing to these properties, **1** should be applicable to the detection of biologically relevant intracellular zinc ions. Rat pancreatic β-cells (Rin-m) were used to test this proposal since they are known to contain relatively high concentrations of intrinsic zinc ions.[3] The cells were cultured in DMEM and then treated with 100 μM **1** for 30 min without the addition of external zinc ions. The results of fluorescence microscopy experiments demonstrate that intracellular zinc ions in β-cells can be fluorescently detected by using this method (Fig. 7c). In addition, the results reveal that cells treated with both **1** (100 μM **1** for 30 min) and external zinc ions (100 μM $ZnCl_2$ for 20 min) have a similar fluorescence response as those treated with **1** only (Fig. 7d). These findings clearly demonstrate that an NBD-based probe **1** can be used for the detection of biologically relevant zinc ions in cells.

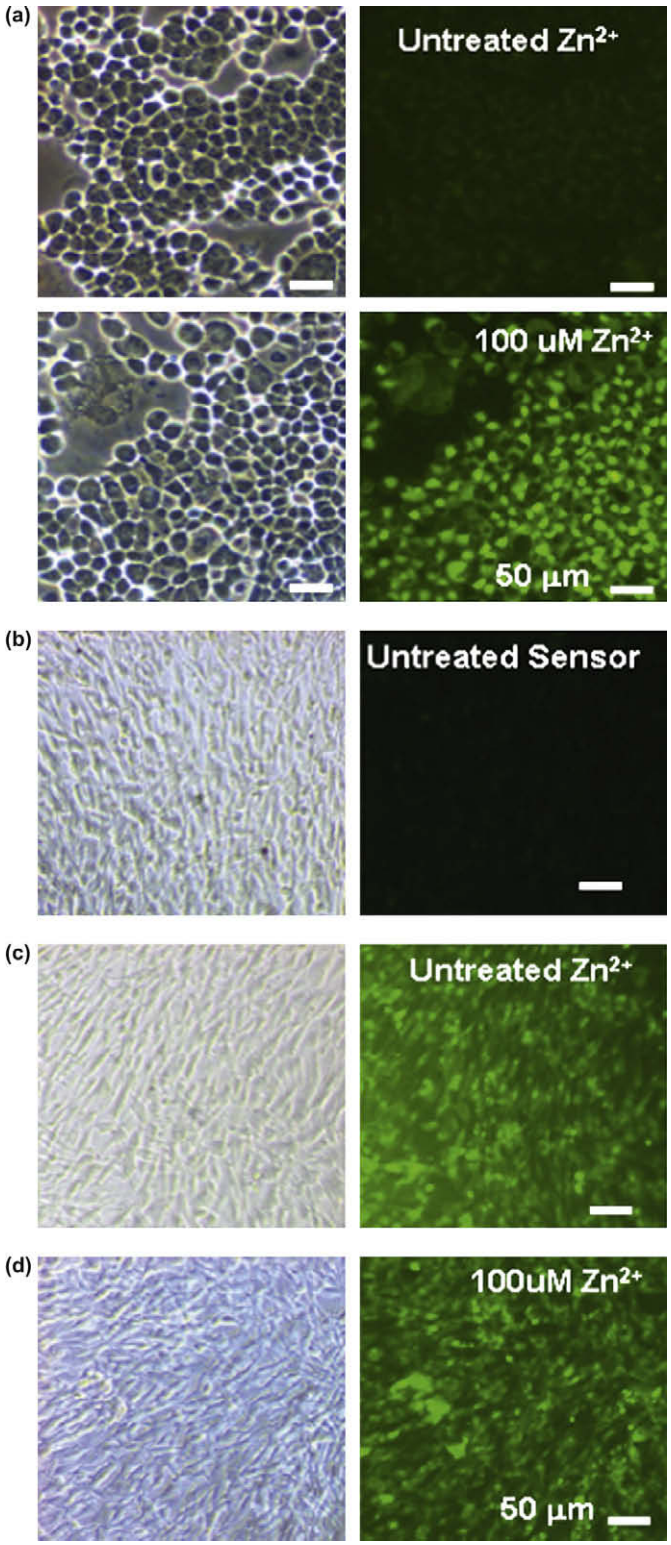

Figure 7. Images of cells incubated with 100 μM **1** and 100 μM Zn^{2+}. (a) Images of Neuro-2a cells incubated with **1** in the absence (top) and presence (bottom) of external Zn^{2+} (100 μM). (b) Images of pancreatic β-cells untreated with **1** and Zn^{2+}. (c) Images of pancreatic β-cells treated only with **1**. (d) Images of pancreatic β-cells treated with both **1** and $ZnCl_2$.

3. Conclusion

In conclusion, this effort has led to the design and synthesis of the new NBD-based fluorescent sensor **1** that can be used for the detection of Zn^{2+}. This displays a selective fluorescent enhancement and colorimetric change with Zn^{2+} ions in aqueous solution. The binding mode of probe **1** with Zn^{2+} was probed by using NMR and CV experiments. Furthermore, the practical use of this probe is demonstrated by its application to the detection of Zn^{2+} ions in pancreatic β-cells. The findings summarized above should serve as the foundation for design and fabrication of new chemosensors.

4. Experimental

4.1. General methods

Unless otherwise noted, materials were obtained from commercial suppliers and were used without further purification. Flash chromatography was carried out on silica gel 60 (230–400 mesh ASTM; Merck). Thin layer chromatography (TLC) was carried out using Merck 60 F_{254} plates with a thickness of 0.25 mm. Preparative TLC was performed using Merck 60 F_{254} plates with a thickness of 1 mm. Melting points were measured using a Büchi 530 melting point apparatus, and are uncorrected. ^1H NMR and ^{13}C NMR spectra were recorded using Bruker 250. Chemical shifts were expressed in parts per million and coupling constants (*J*) in hertz. Mass spectra were obtained using a JMS-HX 110A/110A Tandem Mass Spectrometer (JEOL). UV absorption spectra were obtained on UVIKON 933 Double Beam UV/VIS Spectrometer. Fluorescence emission spectra were obtained using RF-5301/PC Spectrofluorophotometer (Shimadzu).

4.2. Synthesis

4.2.1. Compound **3**

Compound **3** was synthesized by using a modification of the reported procedure (Ref. 10). To a solution of 2.6 mL of ethane-1,2-diamine (38 mmol) in 20 mL of methanol was added 7.4 mL (76 mmol) of 2-pyridinecarboxaldehyde. After stirring for 5 h at reflux, the solution was cooled to room temperature. $NaBH_4$ (4 g, 106 mmol) in 10 mL of methanol was added and the resulting solution was stirred at reflux overnight and concentrated in vacuo. An aqueous solution of the residue was extracted with $CHCl_3$. Concentration of the $CHCl_3$ extracts gave 10 g (86%) of **3** as an oil. ^1H NMR ($CDCl_3$, 250 MHz) δ 2.07 (s, 2H, NH), 2.79 (s, 4H), 3.88 (s, 4H), 7.11 (t, J=6.2 Hz, 2H), 7.28 (d, J=8.2 Hz, 2H), 7.59 (t, J=8.5 Hz, 2H), 8.50 (d, J=4.8 Hz, 2H). ^{13}C NMR ($CDCl_3$, 62.5 MHz) δ 49.10, 55.21, 121.86, 122.21, 136.40, 149.26, 159.92.

4.2.2. Compound **2**

To a solution of 450 mg (1.9 mmol) *N*,*N*′-bis(2-pyridylmethyl)-ethane-1,2-diamine (**3**) in 20 mL dry THF was added slowly 200 mg (1 mmol) NBD–Cl (**4**). The mixture was stirred at room temperature for 2 h. After the reaction was complete (monitored by TLC), the solution was concentrated in vacuo giving a residue, which was subjected to column chromatography (SiO_2, CH_2Cl_2/MeOH, 25:1, v/v) to give 405 mg (86%) **2** as a red semisolid. ^1H NMR ($CDCl_3$, 250 MHz) δ 2.30 (s, 1H, NH), 3.06 (t, J=6.5 Hz, 2H), 3.87 (s, 2H), 4.23 (s, 2H), 5.22 (s, 2H), 6.17 (d, J=9.0 Hz, 1H), 7.15 (m, 4H), 7.57 (m, 2H), 8.26 (d, J=9.0 Hz, 1H), 8.44 (d, J=4.6 Hz, 1H). ^{13}C NMR ($CDCl_3$, 62.5 MHz) δ 29.68, 46.92, 54.95, 58.82, 102.48, 121.35, 122.17, 122.26, 122.74, 122.96, 135.34, 136.59, 137.14, 144.54, 144.78, 145.71, 149.32, 149.91, 154.92, 159.04. HRMS (ESI) calcd for $C_{20}H_{20}N_7O_3$ [MH^+] 406.4179, found 406.4182.

4.2.3. Compound **1**

To a solution of 210 mg (0.52 mmol) (**2**) in 15 mL dry acetonitrile was added 116 mg (0.67 mmol) 2-(bromomethyl)pyridine hydrobromide and 280 mg K_2CO_3. The mixture was stirred at 60 °C for 2 h under nitrogen. After the reaction was complete (monitored by

TLC), the solution was concentrated in vacuo giving a residue, which was subjected to alumina column chromatography (CH_2Cl_2/MeOH=20:1) to give 223 mg (92%) **1** as a brown solid. ^1H NMR ($CDCl_3$, 250 MHz) δ 3.04 (t, J=6.5 Hz, 2H), 3.89 (s, 4H), 4.16 (s, 2H), 5.23 (s, 2H), 6.06 (d, J=9.0 Hz, 1H), 7.15 (m, 4H), 7.36 (d, J=7.5 Hz, 2H), 7.58 (m, 3H), 8.24 (d, J=9.0 Hz, 1H), 8.44 (m, 3H). ^{13}C NMR ($CDCl_3$, 62.5 MHz) δ 50.34, 52.38, 58.94, 60.82, 102.18, 121.23, 122.29, 122.43, 122.89, 123.35, 135.23, 136.49, 137.03, 144.30, 144.72, 145.27, 149.20, 149.94, 155.11, 158.47. HRMS (ESI) calcd for $C_{26}H_{25}N_8O_3$ [M+H$^+$] 497.5285, found 497.5290.

4.3. Preparation of fluorometric metal ion titration solutions

Stock solutions (1 mM) of the perchlorate salts of Ag^+, Ca^{2+}, Cd^{2+}, Co^{2+}, Cs^+, Cu^{2+}, Fe^{2+}, Fe^{3+}, Hg^{2+}, K^+, Li^+, Mg^{2+}, Mn^{2+}, Na^+, Ni^{2+}, Pb^{2+}, and Zn^{2+} ions in distilled water were prepared. Stock solutions of host (0.01 mM) in DMSO were also prepared. Test solutions were prepared by placing 4–40 μL of the probe stock solution into a test tube, adding an appropriate aliquot of each metal stock, and diluting the solution to 4 mL with 0.1 M HEPES (pH 7.2). For all measurements, excitation was at 356 nm. Both excitation and emission slit widths were 3 nm or 5 nm.

4.4. Cyclic voltammetry (CV) measurements

CV experiments were carried out in CH_3CN containing 1 mM electroactive compound and 0.1 M tetrabutylammonium perchlorate (TBAP) at room temperature using a BAS 100B electrochemical analyzer. A platinum disk (Φ=1.6 mm), platinum wire, and Ag|$AgNO_3$ (0.1 M) were used as the working, counter, and reference electrodes, respectively. The potential values shown in this text were calibrated versus the ferrocene/ferrocenium (Fc|Fc$^+$) redox couple, and then corrected to the saturated calomel electrode (SCE) on the basis of Fc|Fc$^+$ redox potential as 0.39 V versus SCE.

4.5. In vivo fluorescence experiment

Neuro-2a neuroblastoma cells (ATCC: American Type Culture collection, Manassas, VA) were cultured in culture media (DMEM supplemented with 10% FBS, 50 units/mL of penicillin and 50 μg/mL of streptomycin) at 37 °C in a humidified incubator. The cells were incubated with 100 μM $ZnCl_2$ in culture media for 20 min at 37 °C. After washing with PBS to remove the remaining zinc ions, the treated cells were incubated with 100 μM **1** in culture media for 30 min at 37 °C. The incubated cells were imaged by fluorescence microscopy (Nikon Eclipse TE2000, FITC filter). Pancreatic β-cells (Rin-m cells, ATCC: American Type Culture collection, Manassas, VA) were cultured in culture media (DMEM supplemented with 10% FBS, 50 units/mL of penicillin and 50 μg/mL of streptomycin) at 37 °C in a humidified incubator. The cells were incubated either with or without 100 μM $ZnCl_2$ in culture media for 20 min at 37 °C. After washing with PBS to remove the remaining zinc ions, the treated cells were incubated with 100 μM **1** in culture media for 30 min at 37 °C. The incubated cells were imaged by fluorescence microscopy.

Acknowledgements

This work was supported by grants from the NRL program (R04-2007-000-2007-0 and R0A-2005-000-10027-0), the SRC program of KOSEF/MEST (R11-2005-008 and R11-2000-070), and WCU (R31-2008-000-10010-0) program. G.-H.K and M.J.C. also thank the BK21 program (KRF). Mass spectral data were obtained from the Korea Basic Science Institute (Daegu) on a Jeol JMS 700 high resolution mass spectrometer.

Supplementary data

Supplementary data associated with this article can be found in the online version, at doi:10.1016/j.tet.2009.01.035.

References and notes

1. (a) Callan, J. F.; de Silva, A. P.; Magri, D. C. *Tetrahedron* **2005**, *61*, 8551; (b) de Silva, A. P.; Gunaratne, H. Q. N.; Gunnlaugsson, T. A.; Huxley, T. M.; McCoy, C. P.; Rademacher, J. T.; Rice, T. E. *Chem. Rev.* **1997**, *97*, 1515; (c) Czarnik, A. W. *Acc. Chem. Res.* **1994**, *27*, 302; (d) Kim, J. S.; Quang, D. T. *Chem. Rev.* **2007**, *107*, 3780; (e) Kim, H. N.; Lee, M. H.; Kim, H. J.; Kim, J. S. *Chem. Soc. Rev.* **2008**, *37*, 1465.
2. (a) Vallee, B. L.; Falchuk, K. H. *Physiol. Rev.* **1993**, *73*, 79; (b) Berg, J. M.; Shi, Y. *Science* **1996**, *271*, 1081.
3. Chausmer, A. B. *J. Am. Coll. Nutr.* **1998**, *17*, 109.
4. Quarterman, J.; Mills, C. F.; Humphries, W. R. *Biochem. Biophys. Res. Commun.* **1966**, *25*, 354.
5. Frederickson, C. J.; Koh, J. Y.; Bush, A. I. *Nat. Rev. Neurosci.* **2005**, *6*, 449.
6. (a) Qian, W. J.; Aspinwall, C. A.; Battiste, M. A.; Kennedy, R. T. *Anal. Chem.* **2000**, *72*, 711; (b) Jindal, R. M.; Taylor, R. P.; Gray, D. W.; Esmeraldo, R.; Morris, P. J. *Diabetes* **1992**, *41*, 1056; (c) Crivat, G.; Kikuchi, K.; Nagano, T.; Priel, T.; Hershfinkel, M.; Sekler, I.; Rosenzweig, N.; Rosenzweig, Z. *Anal. Chem.* **2006**, *78*, 5799; (d) Chang, C. J.; Jaworski, J.; Nolan, E. M.; Sheng, M.; Lippard, S. J. *Proc. Natl. Acad. Sci. U.S.A.* **2004**, *101*, 1129; (e) Kiyose, K.; Kojima, H.; Urano, Y.; Nagano, T. *J. Am. Chem. Soc.* **2006**, *128*, 6548; (f) Wu, Y.; Peng, X.; Guo, B.; Fan, J.; Zhang, Z.; Wang, J.; Cui, A.; Gao, Y. *Org. Biomol. Chem.* **2005**, 1387; (g) Parkesh, R.; Lee, T. C.; Gunnlaugsson, T. *Org. Biomol. Chem.* **2007**, 310; (h) Joshi, B.; Cho, P. W.-M.; Kim, J. S.; Yoon, J.; Lee, K.-H. *Bioorg. Med. Chem. Lett.* **2007**, *17*, 6425; (i) Park, M. S.; Swamy, K. M. K.; Lee, Y. J.; Lee, H. N.; Jang, Y. J.; Moon, Y. H.; Yoon, J. *Tetrahedron Lett.* **2006**, *47*, 8129.
7. (a) Xu, Z.; Qian, X.; Cui, J. *Org. Lett.* **2005**, *7*, 3029; (b) Kwon, J. Y.; Jang, Y. J.; Lee, Y. J.; Kim, K.-M.; Seo, M.-S.; Nam, W.; Yoon, J. *J. Am. Chem. Soc.* **2005**, *127*, 10107; (c) Swamy, K. M. K.; Ko, S.-K.; Kwon, S. K.; Lee, H. N.; Mao, C.; Kim, J.-M.; Lee, K.-H.; Kim, J.; Shin, I.; Yoon, J. *Chem. Commun.* **2008**, 5915; (d) Chen, X.; Nam, S.-W.; Jou, M. J.; Kim, Y.; Kim, S.-J.; Park, S.; Yoon, J. *Org. Lett.* **2008**, *10*, 5235; (e) Soh, J. H.; Swamy, K. M. K.; Kim, S. K.; Kim, S.; Lee, S.-H.; Yoon, J. *Tetrahedron Lett.* **2007**, *48*, 5966.
8. (a) Scheller, F. W.; Schubert, F.; Fedrowitz, J. *Frontiers in Biosensors II. Practical Applications*; Birkhauser: Berlin, 1997; (b) Wang, W.; Gao, S.; Wang, B. *Curr. Org. Chem.* **2002**, *6*, 1285.
9. During the preparation of our manuscript, an NBD based sensor for zinc ion was recently reported; Jiang, W.; Fu, Q.; Fan, H.; Wang, W. *Chem. Commun.* **2008**, 259.
10. Mialane, P.; Nivorojkine, A.; Pratviel, G.; Azéma, L.; Slany, M.; Godde, F.; Simaan, A.; Banse, F.; Kargar-Grisel, T.; Bouchoux, G.; Sainton, J.; Horner, O.; Guilhem, J.; Tchertanova, L.; Meunier, B.; Girerd, J. *Inorg. Chem.* **1999**, *38*, 1085.
11. (a) Association constants were obtained using the computer program ENZFITTER, available from Elsevier-BIOSOFT, 68 Hills Road, Cambridge CB2 1LA, United Kingdom. (b) Conners, K. A. *Binding Constants, The Measurement of Molecular Complex Stability*; Wiley: New York, NY, 1987.
12. Swamy, K. M. K.; Park, M. S.; Han, S. J.; Kim, S. K.; Kim, J. H.; Lee, C.; Bang, H.; Kim, Y.; Kim, S.-J.; Yoon, J. *Tetrahedron* **2005**, *61*, 10227.